Inelastic processes in collisions of H^+ ions with C, N, O, and Si atoms below 1 keV

M. Kimura
School of Allied Health Sciences, Yamaguchi University, Ube, Yamaguchi 755, Japan
and Department of Physics, Rice University, Houston, Texas 77251

J. P. Gu, G. Hirsch, and R. J. Buenker
Theoretische Chemie, Bergische Universität-Gesamthochschule Wuppertal, D-42097 Wuppertal, Germany
(Received 29 August 1996)

Electron capture in collisions of C, N, O, and Si atoms with H^+ ions is studied theoretically based on a molecular representation within a fully quantum framework by including six molecular channels both for the ground and excited states for the $[H^+ + C]$ system, and four channels for the ground-state $[H^+ + N]$ and $[H^+ + O]$ systems. For the $[H^+ + Si]$ system, we employed the molecular representation both in fully quantum and semiclassical frameworks to investigate electron capture at higher energy as well. The *ab initio* potential curves and nonadiabatic coupling matrix elements for all these systems are obtained from multireference single- and double-excitation configuration interaction calculations. For all systems, the effect of excited atoms on electron capture is examined in addition to that from the ground state. Because of a small asymptotic energy defect (near-resonant processes) between the initial and closest electron capture channels for almost all systems, electron capture cross sections from the ground-state atoms are large with values of approximately $10^{-16}-10^{-15}$ cm^2 for all systems at above 100 eV. Corresponding rate coefficients are found to be much smaller than those previously reported for the NH^+ and OH^+, but, on the contrary, found to be larger by a few orders of magnitude than the previously estimated value for the SiH^+ system. Those from excited states are also found to be extremely efficient for all cases. [S1050-2947(97)05803-4]

PACS number(s): 34.10.+x, 34.70.+e, 34.20.−b

I. INTRODUCTION

Electron capture reactions resulting from collisions of protons with carbon, nitrogen, oxygen, and silicon atoms are known to play an important role in the Earth's atmosphere [1,2], interstellar space [3], and astrophysical plasmas [4], and to be fundamental for a deeper understanding of other relevant applied fields such as fusion research and ion implantation in plasma chemistry [5]. Yet, accurate rates for these processes are rarely known except for some crude and limited attempts for evaluation, and certainly more reliable results are urgently needed. Rate coefficients for $[H^+ + N]$ and $[H^+ + O]$ were theoretically evaluated by Steigman *et al.* [6] and Field and Steigman [7], respectively, based on an orbiting approximation with corresponding values of 2.5×10^{-14} cm^3/s and 7.4×10^{-10} cm^3/s, at 1000 K, respectively. Chambaud *et al.* [8] carried out a more rigorous study on electron capture in $[H^+ + O]$ collisions using a molecular orbital method with the spin-orbit coupling as a driving force and determined the rate as 4.8×10^{-10} cm^3/s at 1000 K, which is in reasonable accord with the value by Field and Steigman [7]. But at lower temperature, both values deviate by several orders of magnitude. There is no large-scale theoretical study on $[H^+ + C]$ and $[H^+ + N]$ collision systems except for an exploratory calculation by Butler and Dalgarno [9] for the $[N^+ + H]$ system.

Except for some experiments on the $[H^+ + O]$ collision system by Stebbings *et al.* [1], Fehsenfeld and Ferguson [10], and more recently by Van Zyl and Stephen [11] and Thompson *et al.* [12], there has been no experimental activity to our knowledge for $[H^+ + C]$ and $[H^+ + N]$ systems. The situation is no better for the $[H^+ + Si]$ collisions. Specifically, Baliunas and Butler [13] examined the effect of electron capture for silicon spectral lines and gave the approximate rate coefficient as 10^{-11} cm^3/s for a temperature around 10 000 K, based on a simple model. Our earlier calculations [14] suggested that the rate coefficient for electron capture in collisions of H^+ ions with Si atoms may reach as large as 10^{-8} cm^3/s at 10 000 K.

In this paper, we attempt to investigate collision dynamics, and to evaluate electron-capture cross sections and corresponding rate coefficients for these four target atoms rigorously based on a molecular representation within a fully quantal framework for HC^+, HN^+, and HO^+ and within both semiclassical and fully quantal frameworks for HSi^+. The processes we have studied are as follows, with corresponding asymptotic energy defects given between the closest states.

(i) For the ground state,

$$H^+ + C(^3P) \rightarrow H + C^+(^2P) + 2.33 \text{ eV}, \quad (1a)$$

$$H^+ + N(^4S) \rightarrow H + N^+(^3P) - 0.95 \text{ eV}, \quad (1b)$$

$$H^+ + O(^3P) \rightarrow H + O^+(^4S) - 0.02 \text{ eV}, \quad (1c)$$

$$H^+ + Si(^3P) \rightarrow H + Si^+(^4P) + 0.138 \text{ eV}. \quad (1d)$$

Note that the CH^+ and SiH^+ systems are exothermic and the NH^+ and OH^+ systems are endothermic reactions with very small asymptotic energy separations: near resonant electron capture.

(ii) For the excited state,

$$H^+ + C(^1D) \rightarrow H + C^+(^2P) + 3.59 \text{ eV}, \quad (2a)$$

TABLE I. Types and exponents α of atomic orbitals added to the $(13s8p)/[7s4p]$ basis sets of Refs. [20–22] for the carbon, nitrogen, and oxygen atoms, respectively.

C		N		O	
Type	$\alpha(a_0^{-2})$	Type	$\alpha(a_0^{-2})$	Type	$\alpha(a_0^{-2})$
s	0.023	s	0.0532	s	0.032
		s	0.021		
p	0.021	p	0.0475	p	0.028
		p	0.0188		
d	0.920	d	1.082	d	1.324
d	0.256	d	0.343	d	0.445

$$H^+ + N(^2D) \rightarrow H + N^+(^1D) - 0.47 \text{ eV}, \quad (2b)$$

$$H^+ + O(^1D) \rightarrow H + O^+(^2D) - 1.38 \text{ eV}, \quad (2c)$$

$$H^+ + Si(^1D) \rightarrow H + Si^+(^3D) - 0.628 \text{ eV}. \quad (2d)$$

The metastable states considered here are $C(^1D)$, $N(^2D)$, $O(^1D)$, and $Si(^1D)$, which are separated from the corresponding ground states only by 1.26, 2.38, 1.96, and 0.78 eV for CH^+, NH^+, OH^+, and SiH^+, respectively, and, hence these excited atoms are expected to be abundantly produced and be present in various environments at high temperature such as in intersteller space where high-energy γ rays and charged particles constantly interact with constituent atoms and molecules. A mixture of both ground and metastable atoms makes the analysis of spectroscopic data more complicated for these atoms and hence precise knowledge of collision dynamics for these atomic states is highly desirable.

II. THEORETICAL MODEL

The present molecular calculations are methodologically similar to our earlier work on the various diatomic systems reported [15,16] for the determination of molecular electronic states. For collision dynamics, both semiclassical and quantal close-coupling methods have been used extensively by this group [15,16] and others [8,9] and hence only a short summary of electronic-state and collision dynamics calculations is given here [17–19].

A. Molecular states and couplings

The atomic orbital (AO) basis sets employed in the present $H^+ - C$, N, O calculations consist of contracted Cartesian Gaussian functions. The $(8s2p)$ basis of Lie and Clementi [20] for the hydrogen atom is contracted to $[5s2p]$ and augmented by one s- and one p-type diffuse function with exponents $\alpha_s = 0.0195 a_0^{-2}$ and $\alpha_p = 0.042 a_0^{-2}$. For the NH^+ calculations an additional d-type function with $\alpha_d = 1.1 a_0^{-2}$ has been added as well to describe polarization effects. The basis sets for the carbon-nitrogen-oxygen atoms are from van Duijneveldt [21,22], with the contraction scheme of Lie and Clementi [20] as tabulated in Ref. [22]. These $(13s8p)/[7s4p]$ basis sets have been augmented with several s,p, and d functions as listed in Table I. The resulting basis sets are thus of $(14s9p2d)/[8s5p2d]$ quality for carbon and oxygen and of $(15s10p2d)/[9s6p2d]$ quality for nitrogen. The self-consistent field (SCF) calculations are then carried out for respective electronic states of the three molecules, i.e., $X\ ^1\Sigma^+$ for CH^+, $a\ ^4\Sigma^-$ for NH^+, and $X\ ^3\Sigma^-$ for OH^+. The resulting SCF molecular orbitals (MOs) form the orthonormal one-electron basis for the subsequent configuration-interaction (CI) treatments. Generally more than 30 geometries have been calculated between $r = 1.0 a_0$ and $10.0 a_0$ for these systems. In the case of CH^+ and OH^+ additional calculations have been made at $r = 20.0 a_0$. The multireference single- and double-excitation (MRD-CI) configuration interaction method is employed with configuration selection and perturbative energy corrections [23]. A set of reference configurations is chosen based on a preliminary scan of the wave functions of the lowest roots of a given symmetry at representative internuclear distances. Selection thresholds of $T = 3.0 \mu E_h$ (3.0×10^{-6} hartree) (for NH^+ and OH^+) and $T = 1.0 \mu E_h$ (1.0×10^{-6} hartree) (for CH^+) are employed to divide the generated configurations into two sets based on their ability to lower the total energy of a given root relative to that obtained in the small reference secular equations. The number of the reference configurations and the roots selected for each symmetry are given in Table II. The calculations are carried out in the C_{2v} subgroup of the $C_{\infty v}$ point group, but the MOs themselves transform according to the linear irreducible representations, making identification of the resulting CI eigenfunctions straightforward. The A_1 irreducible representation (C_{2v}) yields Σ^+ and Δ states, while A_2 gives Σ^- and Δ states; the $B_{1,2}$ results correspond to Π states.

TABLE II. Number of reference configurations N_{ref} and number of roots N_{root} treated in each irreducible representation.

CH^+		NH^+		OH^+	
States	$N_{\text{ref}}/N_{\text{root}}$	States	$N_{\text{ref}}/N_{\text{root}}$	States	$N_{\text{ref}}/N_{\text{root}}$
$^1A_1$	89/5	$^2A_1$	75/6	$^1A_1$	92/6
$^1B_{1,2}$	63/3	$^2B_{1,2}$	56/5	$^1B_{1,2}$	61/4
$^1A_2$	63/2	$^2A_2$	51/5	$^1A_2$	59/4
$^3A_1$	87/2	$^4A_1$	16/1	$^3A_1$	96/3
$^3B_{1,2}$	69/4	$^4B_{1,2}$	40/2	$^3B_{1,2}$	80/4
$^3A_2$	55/3	$^4A_2$	33/3	$^3A_2$	61/5
$^5B_{1,2}$	56/2				
$^5A_2$	64/3				

The CI treatment itself is carried out with computer programs employing the table CI algorithm [24] for efficient handling of the various open shell cases, which arise because of the single and double substitutions relative to the reference configurations. The sum of squared coefficients of the reference configurations Σc_p^2 for each root treated is an indication of the quality of the choice of the reference species in each case. Typically values of 0.95 or larger are found, which is a satisfactory range for CI treatments with only six to eight active electrons. The Σc_p^2 values are also employed in the multireference analogue to the Davidson correction [25,26] to the energy of each root in order to estimate the effect of higher excitations and therefore to obtain the corresponding full CI energy to a good approximation.

The finite difference technique [27–29] has been employed to obtain radial coupling matrix elements between

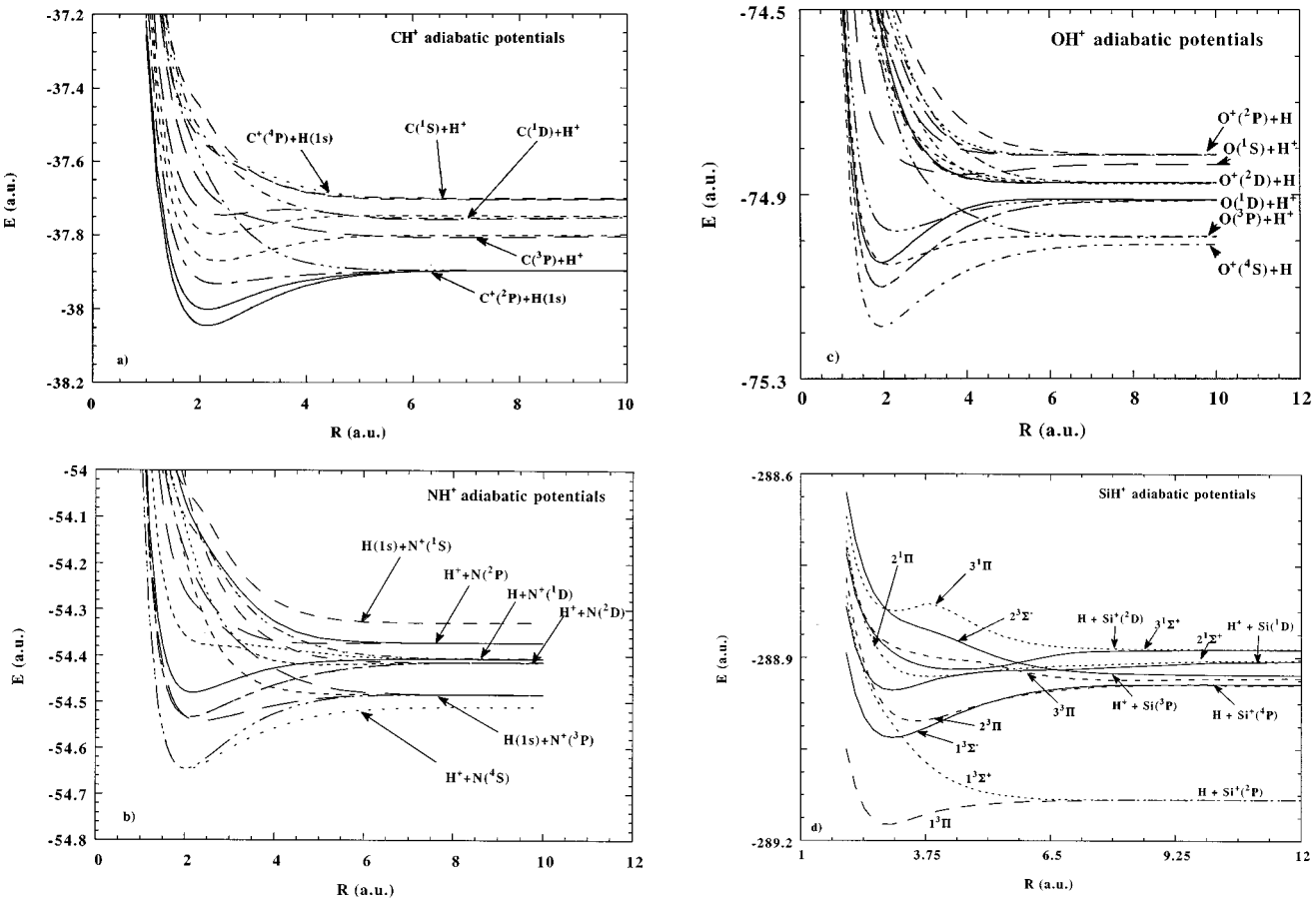

FIG. 1. Adiabatic potentials of the (a) CH^+, (b) NH^+, (c) OH^+, and (d) SiH^+ systems.

selected states of the same symmetry, whereas rotational coupling matrix elements as well as electric dipole transition moments have been computed by employing appropriate pairs of CI eigenfunctions for which nonzero results are allowed by symmetry. Additional computational details for SiH^+ may be found in the previous work [14].

B. Collision dynamics

1. Semiclassical approach

A semiclassical MO expansion method with a straight-line trajectory of the incident ion was employed to study the collision dynamics above 30 eV [19]. In this approach, the relative motion of heavy particles is treated classically by using a straight-line trajectory, while electronic motion is treated quantum mechanically. The total scattering wave function is expanded in terms of products of a molecular electronic state and atomic-type electron translation factors (ETFs), whereby the inclusion of the ETF ensures that the correct asymptotic scattering boundary condition of the scattering equations is satisfied. Substituting the total wave function into the time-dependent Schrödinger equation and retaining the ETF correction up to first order in the relative velocity between the collision partners, we obtain a set of first-order coupled equations in time t. This approximation of retaining the first order of relative velocity is expected to be valid in the present energy region. Transitions between the molecular states are driven by nonadiabatic couplings. By solving the coupled equations numerically, we obtain the scattering amplitudes for transitions: the square of the amplitude gives the transition probability, and integration of the probability over the impact parameter gives the cross section. The molecular states included in the dynamical calculations are the two sets of states, shown in Fig. 1(d), separating to $[H^+ + Si(^3P)]$ $(2\,^3\Sigma^-, 3\,^3\Pi)$, $[H + Si^+(^4P)]$ $(1\,^3\Sigma^-, 2\,^3\Pi)$, $[H + Si^+(^2P)]$ $(1\,^3\Sigma^+, 1\,^3\Pi)$ for electron capture from the initial ground state, and $[H^+ + Si(^1D)]$ $(2\,^1\Sigma^+, 2\,^1\Pi)$, $[H + Si^+(^2D)]$ $(3\,^1\Sigma^+, 3\,^1\Pi)$ for electron capture from the initial excited state.

2. Quantum approach

A fully quantum-mechanical representation of the MO expansion method is employed, that is, the total wave function is expanded in products of molecular electronic and nuclear wave functions and the ETFs, and is substituted into the time-independent Schrödinger equation to yield a set of second-order coupled equations. By solving the coupled equations numerically, the scattering s matrix is extracted. From the standard procedure, the s matrix can be related to a transition probability and hence cross section. Molecular states included in the present calculation are as follows: (i) for the $[H^+ + C]$ system, for the ground-state initial channel $[H^+ + C(^3P)]$; Σ^-, Π, electron capture $[H + C^+(^4P)]$; Σ^- and $[H + C^+(^2P)]$; Σ^+, Π, and for excited states, the initial $[H^+ + C^*(^1D)]$; Σ^+, Π, electron capture $[H + C^+(^2P)]$; Σ^+, Π, and target excitation $[H^+ + C^*(^1S)]$; Σ^+; (ii) for the $[H^+ + N]$ system, the initial $[H^+ + N(^4S)]$; $X\,^4\Sigma^-$, electron capture $[H + N^+(^3P)]$ and target excitation $[H^+ + N(^4P)]$;

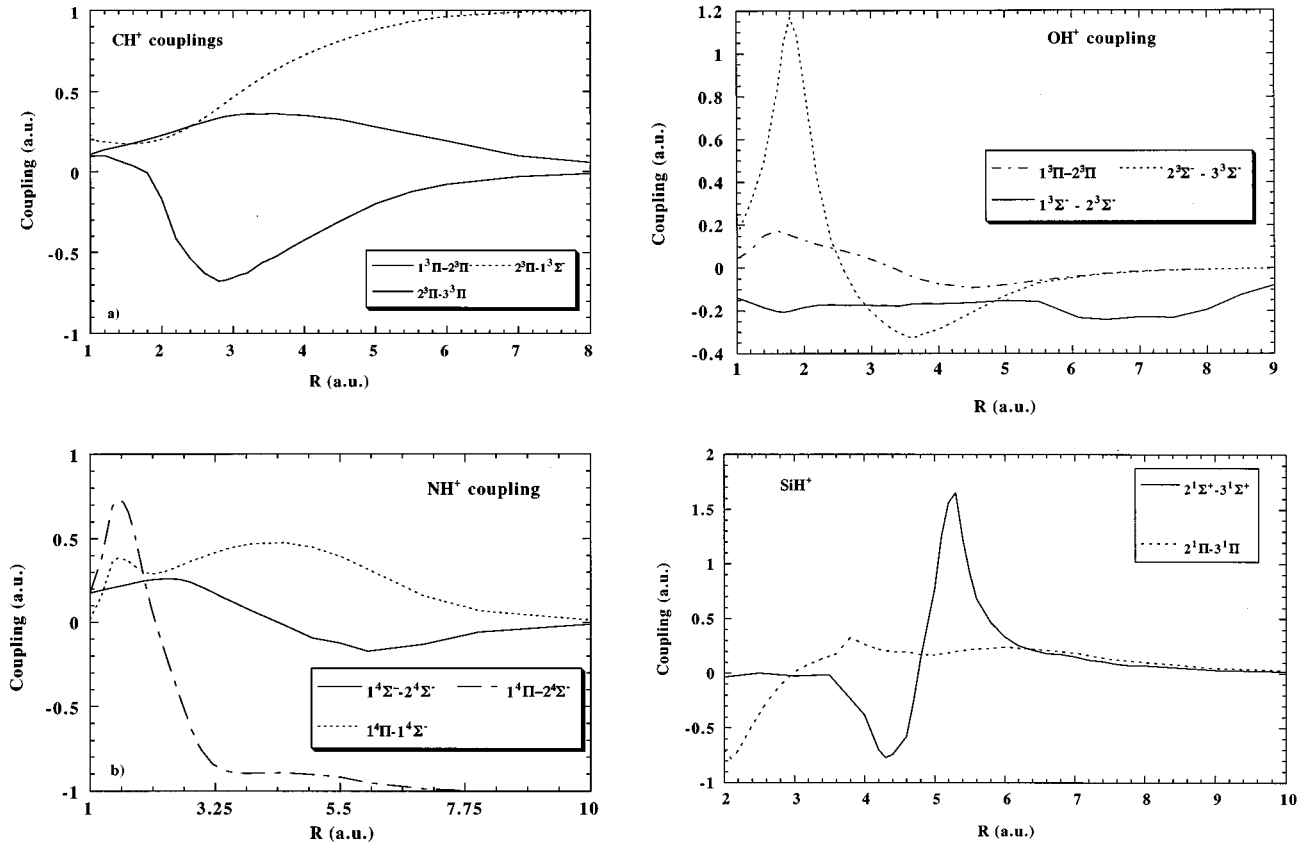

FIG. 2. Representative nonadiabatic radial and angular coupling matrix elements for (a) CH^+, (b) NH^+, (c) OH^+, and (d) SiH^+ systems.

(iii) for the $[H^+ + O]$ system, the initial $[H^+ + O(^3P)]$; $X\ ^3\Sigma^-$ and electron capture $[H + O^+(^4S)]$; $2\ ^3\Sigma^-$; and for excited states, the initial $[H^+ + O(^1D)]$; $1^1\Sigma^+$, $1^1\Pi$, and electron capture $[H + O^+(^2D)]$; $1^1\Sigma^-$, $2^1\Pi$; (iv) for the $[H^+ + Si]$ system, then initial $[H^+ + Si(^1D)]$; $2^1\Sigma^+$, $2^1\Pi$, and electron capture $[H + Si^+(^2D)]$; $3^1\Sigma^+$,$3^1\Pi$. Furthermore, contributions from higher Σ states were also examined for selected cases to estimate the degree of the convergence of the cross section.

III. RESULTS

A. Adiabatic potentials and corresponding coupling matrix elements

The calculated adiabatic potentials and corresponding representative radial and angular coupling matrix elements are displayed in Figs. 1(a)–1(d) and Figs. 2(a)–2(d) for CH^+, NH^+, OH^+, and SiH^+, respectively. First, we discuss each system separately and then provide general features common to all. For the CH^+ system as shown in Fig. 1(a), the ground $[H^+ + C(^3P)]$ channel lies above the dominant electron capture $[H + C^+(^2P)]$ channel, whereas all target-excitation $[H^+ + C(^1D, ^1S)]$ channels lie slightly above the ground state. For low-energy collisions below the eV regime, it would be expected that electron capture from the ground state proceeds to form a $C^+(^2P)$ state through both *radiative* and *nonradiative* electron capture driven by a dipole and spin-orbit couplings between the initial ($^3\Sigma^-$ and $^3\Pi$) and electron-capture ($^1\Sigma^+$,$^1\Pi$) and ($^3\Sigma^+$,$^3\Pi$) channels, but as the energy increases to a few tens of eV region, capture may take place primarily to the $^3\Pi$ state in the $[H + C^+(^2P)]$ channel through a radial coupling from the initial $^3\Pi$ state. Note that the $[H^+ + C(^1S)]$ and $[H + C^+(^4P)]$ channels lie very closely and in the figure, both potentials looks nearly identical.

For the NH^+ system in Fig. 1(b), the $[H^+ + N^+(^4S)]$ channel is the ground state with the electron capture $[H + N^+(^3P)]$ channel being nearby. Above this electron capture channel, a series of target excitation channels follows. For OH^+ in Fig. 1(c), the $[H^+ + O(^3P)]$ channel is the lowest level, similarly for the NH^+ system, and then the electron capture $[H + O^+(^4S)]$ channel and the target excitation $[H^+ + O(^1D)]$ channel follow. In the present calculation, the first two of these levels are inverted, but these orders have been changed to match the experimental result in the scattering calculation described below. As Chambaud *et al.* [8] suggested the importance of a transition among different spin states through a spin-orbit coupling, these inter-spin-multiplicity (singlet-triplet) transitions become increasingly important particularly at a point where these potentials for different spin states cross as the collision energy decreases below low-eV region. For the SiH^+ system as shown in Fig. 1(d), it should be noted that the energy splitting between the levels corresponding to the $[H + Si^+(^4P)]$ and $[H^+ + Si(^3P)]$ systems is known experimentally to be only 1112 cm^{-1} and because of this small value, a larger basis set for describing electronic states is required to obtain this splitting reasonably well [14].

Energy defects between the initial ground state and nearest electron capture state are, therefore, 2.3, 0.95, 0.02, and

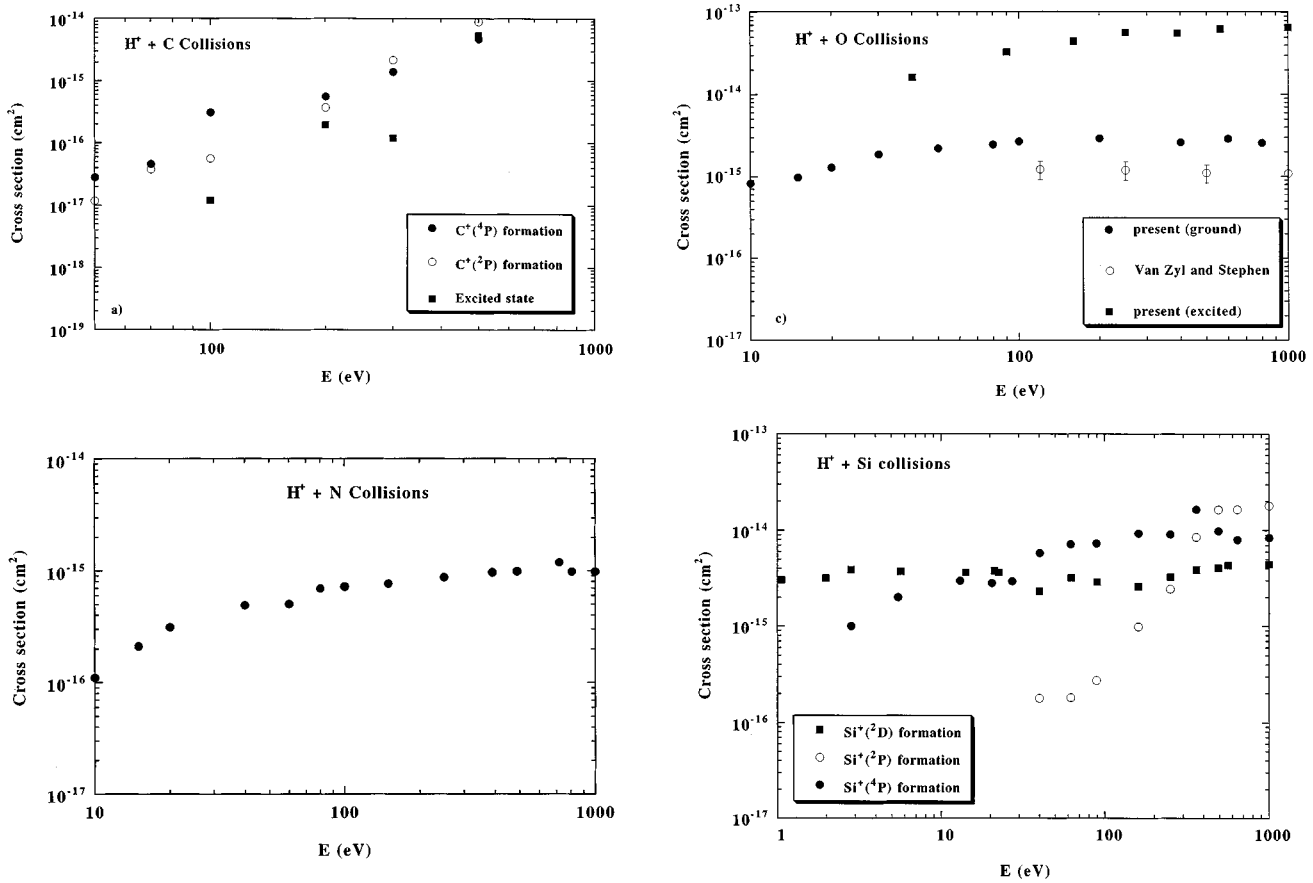

FIG. 3. Electron capture cross sections both from the ground and excited states below 1000 eV for (a) CH^+, (b) NH^+, (c) OH^+, and (d) SiH^+. Present work for all systems: ●. For OH^+, experimental data: open circle, Ref. [11].

0.14 eV for $[H^+ + C]$, $[H^+ + N]$, $[H^+ + O]$, and $[H^+ + Si]$ systems, respectively, while those between the initial excited state and closest electron capture state are 3.6, 0.47, 1.38, and 0.63 eV, respectively, for the same systems. Therefore, we would expect that at the lower end of collision energies studied, electron capture from the ground state dominates for the $[H^+ + N,O,Si]$ systems, but is somewhat weaker for the $[H^+ + C]$ system even though the process is exothermic. For electron capture from the excited state, as the energy slightly increases from the threshold, the number of states available for electron capture quickly increases and for these two N and O target cases, electron capture from the excited atoms is expected to take over that from the ground state. There are several curve crossings among different spin states and, as described earlier, spin-orbit couplings are expected to be a dominant driving force for a spin-forbidden transition at lower energies below a few eV or so.

A dominant coupling mechanism in the present energy range between the initial and closest electron capture channels as examplified in Fig. 2 is considered to be the Demkov-type coupling, i.e., the manifestation of a weak interaction due to the polarization potential, typically low-lying charged-ion collision pair, and as a result, a leading nonadiabatic radial coupling matrix element has a broad weak peak at the internuclear separation where two corresponding potentials approach asymptotically. Typical sizes and shapes of those radial coupling matrix elements are seen in Fig. 2.

B. Electron capture from the ground-state $C(^3P)$, $N(^4S)$, $O(^3P)$, and $Si(^3P)$ atoms

The calculated electron-capture cross sections are illustrated in Figs. 3(a)–3(d) for C, N, O, and Si targets, respectively. As we speculated from the small asymptotic energy defects between the initial and dominant charge-transfer channels for all systems, the cross sections for $C^+(^4P)$, $N^+(^3P)$, $O^+(^4S)$, and $Si^+(^4P)$ formations are found to be large, all with values larger than 10^{-18} cm^2 above the energy of a few tens of eV and rapidly reaching values of nearly 10^{-15} cm^2 around a few hundred eV for all cases. The energy dependence is relatively mild except for near-threshold regions, but all show conspicuous structures due to strong interferences among electron capture channels and the entrance channel. The cross section for $C^+(^2P)$ formation is somewhat weaker in intermediate energy regions due to a less effective coupling scheme with the initial channel, although it rapidly catches up with that of $C^+(^4P)$ formation as the energy increases. The flux is promoted through a series of target excitation channels (a ladder-climbing mechanism), finally reaching the $C^+(^4P)$ channel. Therefore, these target excitation channels are essential for the $C^+(^4P)$ production in this energy range. For N and O targets, energy dependence in capture cross sections is found to be very weak and the cross sections reach nearly constant particularly above 50 eV. $Si^+(^2P)$ formation is similar in magnitude to the $Si^+(^4P)$ cross section above 300 eV, but drops

TABLE III. Representative rate coefficients for electron capture at temperatures above 10 000 K resulting from collisions of H^+ ions with C, N, O, and Si atoms.

	Rate coefficient (cm^3/s) Targets					
Temp. (K)	$C(^3P)$	$N(^4S)$		$O(^3P)$		$Si(^3P)$
10 000		3.51×10^{-11}	5.3×10^{-10} [a]	6.10×10^{-11}	9.1×10^{-10} [b]	1.45×10^{-9}
50 000	2.61×10^{-12}	4.80×10^{-10}		2.91×10^{-9}		7.39×10^{-9}
100 000	2.34×10^{-11}	2.03×10^{-9}		7.02×10^{-9}		1.40×10^{-8}
200 000	2.08×10^{-10}	6.73×10^{-9}		1.39×10^{-8}		2.93×10^{-8}

[a]Reference [6].
[b]Reference [7].

rather sharply below this energy due to a larger energy defect for capture. Oscillatory structures seen in the cross section are rather weak near the threshold region. A peak is seen near the region of 1 keV in the $Si^+(^2P)$ formation while it displays a dip for the $Si^+(^4P)$ formation in the same energy region and this out-of-phase structure in the two cross sections is a manifestation of the interference between these two channels. For both formations, Σ and Π contributions are almost equal except for higher ends of energies studied where the Σ contribution dominates by about a factor of 2, implying the dominance of the Σ-Σ radial coupling.

As stated earlier, to our knowledge there are no comprehensive experimental data for any target in this energy region below 1000 eV for comparison. However, there is one set from a relatively old experiment in the region of 50–10 000 eV [1] and another at thermal energy [10], both for the O target, and more recently, there are experiments above 120 eV [11,12] that can be used for comparison with the present result; the results of Ref. [12] are included in Fig. 3(c). The present results rapidly increase from the threshold and reach a value of 10^{-15} cm^2 at around 20 eV becoming nearly a constant at higher energies. The present value at 100 eV is 2.5×10^{-15} cm^2, which can be compared with the experimental value of 1.1×10^{-15} cm^2 given by Van Zyl and Stephen [12] at 120 eV, somewhat of an overestimation in magnitude, but similar in energy dependence. Since the present study aims to elucidate dynamical aspects in low-energy collisions so that the size of the MO set used is suited for collisions below 100 eV, this may well lead to an overestimation of the cross section for higher energies. Furthermore, below a few eV, radiative capture processes and spin-forbidden transition processes become major dynamical processes [8] over those processes driven by nonadiabatic couplings considered here. Hence, for an accurate description of low-energy collisions, these radiative and spin-forbidden transitions should be included on an equal footing manner.

C. Electron capture from the excited $C(^1D)$, $O(^1D)$, and $Si(^1D)$ atoms

Electron-capture processes from excited atoms of $C(^1D)$, $O(^1D)$, and $Si(^1D)$ atoms by H^+ impact have been examined, as included and exemplified in Fig. 3. For the $O(^1D)$ atom, due to a combination of a small energy defect, the availability of a larger number of channels and the effectiveness of the strong coupling between the initial excited state and electron capture channels, the cross section is found to be large, being weakly dependent on the collision energy and to possess weakly oscillatory structures, and it rapidly reaches the value in the region of 10^{-14} cm^2. For the $C(^1D)$ atom, the situation is somewhat different because many target excitation and deexcitation channels lie closer energetically to the initial excited state [see Fig. 1(a)] and hence, the target excitation processes dominate by far over electron capture at all energies. At 100 eV, for example, the electron-capture cross section is in the neighborhood of 1.0×10^{-17} cm^2 and drops rapidly toward threshold, whereas the excitation cross section is already close to 2×10^{-15} cm^2 and gradually increases to 4×10^{-15} cm^2 at 500 eV. For the $Si(^1D)$ atom, at lower energies below around 20 eV, electron capture from the excited state is larger than that from the ground state, but it gradually takes over the excitation and dominates by nearly an order of magnitude at 1 keV. The Π contribution is dominant in all systems at higher energies due to increasing the diabatic nature of the Σ-Σ radial coupling. Also, as noted for the $O(^1D)$ atom, oscillatory structures are seen in all systems and these oscillatory patterns are due to the multichannel interference oscillation.

D. Rate coefficients

The rate coefficients for electron capture from the ground-state $C(^3P)$, $N(^4S)$, $O(^3P)$, and $Si(^3P)$ and excited $C(^1D)$, $O(^1D)$, and $Si(^1D)$ atoms are calculated and some representative values are given in Table III [30]. The rates for the ground-state atoms increase from less than 10^{-14} cm^3/s at 10 000 K [31] to 2×10^{-11} cm^3/s at 100 000 K for CH^+, 3.5×10^{-12} cm^3/s to 2×10^{-9} cm^3/s for NH^+, 6.1×10^{-11} cm^3/s to 7×10^{-9} cm^3/s for OH^+, and 1.5×10^{-9} cm^3/s to 1.4×10^{-8} cm^3/s for SiH^+. The rate coefficients for NH^+ and OH^+ at 10 000 K determined by Steigman *et al.* [6] and Field and Steigman [7], respectively, are large with values of 5.3×10^{-10} and 9.1×10^{-10} cm^3/s, respectively, which may be compared with the present 3.5×10^{-11} and 6.1×10^{-11} cm^3/s. For the reason described above, the present rates below 10 000 K may be less reliable. It is apparent that the values previously reported are larger by at least an order of magnitude, which results may have an affect on the determination of the ionization structure in interstellar space. The rate coefficients determined in the present study for SiH^+, that is approximately 10^{-9} cm^3/s at

10 000 K, are found to be much larger than that previously estimated by Baliunas and Butler [13] (10^{-11} cm^3/s). Those for the excited atoms are small at low temperatures, but become comparable at higher energies, varying from 2×10^{-11} cm^3/s to 3×10^{-8}/cm^3/s. Knowledge of the large electron-capture rate from the excited state, which exceeds that of the ground state at higher temperatures, may be important for a diagnostic of astrophysical plasma at higher temperatures. Experimental attempts to determine these rates are urgently required to clarify theoretical situations.

IV. CONCLUSION

We have studied electron capture in collisions of C(^3P), N(^4S), O(^3P), and Si(^3P) with H^+ below 1000 eV and found that the cross sections for electron capture from the ground-state O and Si targets reach as high as $\sim10^{-15}$ cm^2 above a few tens of eV and those are relatively smaller for C and N targets because of a larger asymptotic energy defect. Except for the CH^+ case, corresponding rate coefficients have values larger than 10^{-12} cm^3/s at a temperature of 10 000 K. We have also investigated electron capture from excited state C(^1D), O(^1D), and Si(^1D) atoms by H^+ ion impact in the same energy range. We find that the magnitude and energy dependence of both sets of cross sections for each system vary significantly from system to system because of different characteristics of the various adiabatic potentials and corresponding couplings. We have found that the rate coefficients for electron capture from ground-state atoms are small, with a value less than 10^{-10} cm^3/s at 10 000 K for N and O targets, compared to those reported by Steigman *et al.* [6] and Field and Steigman [7], who give 5.3×10^{-10} and 9×10^{-10} cm^3/s, respectively. The rates for the Si target are found to be much larger (with a value of 1.45×10^{-9} cm^3/s) than that estimated earlier as 10^{-11} cm^3/s by Baliunas and Butler [13]. We believe that the electron-capture information may help to provide a more accurate analysis of astrophysical plasma.

ACKNOWLEDGMENTS

This work was supported in part by the Science and Technology Agency (M.K.) and Deutsche Forschungsgemeinschaft in the form of a Forschergruppe and Grant No. Bu 450/7-1. The financial support of the Fonds der Chemischen Industrie is also hereby gratefully acknowledged. M.K. also acknowledges financial support from the National Science Foundation through the Institute of Theoretical Atomic and Molecular Physics, Harvard-Smithsonian Center for Astrophysics when this project was initiated. The authors also wish to thank Professor A. Dalgarno for a useful discussion.

[1] R. F. Stebbings, A. C. H. Smith, and H. Ehrhardt, J. Geophys. Res. **69**, 2349 (1964).
[2] J. A. Rutherford and D. A. Vroom, J. Chem. Phys. **61**, 2514 (1974).
[3] J. H. Black and A. Dalgarno, Astrophys. J. **206**, 132 (1976).
[4] G. E. Geisler, J. Geophys. Res. **72**, 81 (1967).
[5] R. A. Phaneuf, F. W. Meyer, and R. H. McKnight, Phys. Rev. A **17**, 534 (1974).
[6] G. L. Steigman, M. W. Werner, and F. M. Geldon, Astrophys. J. **168**, 373 (1971).
[7] G. B. Field and G. Steigman, Astrophys. J. **166**, 59 (1971).
[8] G. Chambaud, J. M. Launay, B. Levy, P. Millie, E. Roueff, and F. T. Minh, J. Phys. B **13**, 4205 (1980).
[9] S. E. Butler and A. Dalgarno, Astrophys. J. **234**, 765 (1979).
[10] F. C. Fehsenfeld and E. E. Ferguson, J. Chem. Phys. **56**, 3066 (1972).
[11] B. Van Zyl and T. M. Stephen, in *Proceedings of the 17th International Conference on Physics of Electronic and Atomic Collisions*, edited by I. E. McCarthy, W. R. MacGillivray, and M. C. Standage (Griffith University, Brisbane, 1991), p. 437.
[12] W. R. Thompson, M. B. Shah, and H. B. Gilbody, J. Phys. B **29**, 725 (1996).
[13] S. L. Baliunas and S. E. Butler, Astrophys. J. **235**, L45 (1980).
[14] M. Kimura, A. B. Sannigrahi, J. P. Gu, Y. Li, G. Hirsch, R. J. Buenker, and I. Shimamura, Astrophys. J. **473**, 1114 (1996).
[15] M. Kimura, A. B. Sannigrahi, J. P. Gu, H.-P. Liebermann, Y. Li, G. Hirsch, R. J. Buenker, and A. Dalgarno, Phys. Rev. A **50**, 4854 (1994).
[16] M. Kimura, J. P. Gu, Y. Li, G. Hirsch, and R. J. Buenker, Phys. Rev. A **49**, 3131 (1994).
[17] M. Kimura, J. P. Gu, G. Hirsch, and R. J. Buenker, Phys. Rev. A **51**, 2063 (1995).
[18] S. E. Butler, T. G. Heil, and A. Dalgarno, Astrophys. J. **241**, 442 (1980).
[19] M. Kimura and N. F. Lane, in *Advances in Atomic and Molecular Optical Physics*, edited by D. R. Bates and B. Bederson (Academic, New York, 1989), Vol. 26, p. 76.
[20] G. C. Lie and E. Clementi, J. Chem. Phys. **60**, 1275 (1974).
[21] E. B. Van Duijneveldt, IBM Research Report No. RJ945, 1971 (unpublished).
[22] P. Pointer, R. Kari, and I. G. Csizmadia, *Handbook of Gaussian Basis Sets*, Physical Sciences Data Vol. 24 (Elsevier, Amsterdam, 1985), Tables 6.72.2 for CH^+, 7.73.2 for NH^+, and 8.76.2 for OH^+.
[23] R. J. Buenker and S. D. Peyerimhoff, Theor. Chim. Acta **35**, 33 (1974); R. J. Buenker, Int. J. Quantum Chem. **29**, 435 (1986).
[24] R. J. Buenker, in *Proceedings of the Workshop on Quantum Chemistry and Molecular Physics, Wollongong, Australia*, edited by P. Burton (University Press, Wollongong, 1980); R. J. Buenker and R. A. Phillips, J. Mol. Struct. Theorchem. **123**, 291 (1985).
[25] E. R. Davidson, in *The World of Quantum Chemistry*, edited by R. Daudel and B. Pullman (Reidel, Dordrecht, 1974), p. 17.
[26] G. Hirsch, P. J. Bruna, S. D. Peyerimhoff, and R. J. Buenker, Chem. Phys. Lett. **52**, 442 (1977).
[27] C. Galloy and J. C. Lorquet, J. Chem. Phys. **67**, 4672 (1977).
[28] G. Hirsch, P. J. Bruna, R. J. Buenker, and S. D. Peyerimhoff, Chem. Phys. **45**, 335 (1980).
[29] R. J. Buenker, G. Hirsch, S. D. Peyerimhoff, P. J. Bruna, J.

Romelt, M. Bettendorff, and C. Petrongolo, in *Studies in Physical and Theoretical Chemistry*, Current Aspects of Quantum Chemistry Vol. 21, edited by R. Carbo (Elsevier, Amsterdam, 1981), p. 81.

[30] Note that cross-section values calculated at low energies are not suitable for accurately determining the rate coefficient since we were originally concerned with collsions at intermediate energies and hence these values, particularly at low temperatures, are to be considered just for reference purposes. A more thorough study for low-energy collisions below a few-tens of eV is now under way, andwe plan to report comprehensive information on these results elsewhere.

[31] As described in the text, below a few eV, electron capture through radiative transition and capture through the spin-forbidden transition may become dominant. In this study, we have not included these processes and hence the rate coefficiant evaluated for this system below 10 000 K may not be accurate.